Fracture Mechanics of Concrete Structures,
Proceedings FRAMCOS-2, edited by Folker H. Wittmann,
AEDIFICATIO Publishers, D-79104 Freiburg (1995)

DYNAMIC CRACK PROPAGATION IN PMMA

R. Jelínek[1], H.A. Dieterman, and L.J. Sluys
Department of Civil Engineering, Delft University of Technology, The Netherlands

Abstract

A discrete crack approach has been used to model fast crack propagation in prestressed PMMA (poly-methyl-metha-acrylate) plates. The paper is concerned with the comparison of experimental and computational results. The experiments have been carried out on prestressed plates of viscoelastic PMMA material. The plates with a hole have been preloaded and fracture was initiated by a pressure pulse excited through an explosive wire placed at the end of a transfer bar. Cracking starts at the hole and propagates through the material. The photorecording of the fracture process in the plate shows the crack length development in time. From the computational analyses the influence of the fracture parameters - fracture energy, tensile strength and shape of the softening diagram - on the velocity of crack propagation and the size of the cohesive zone was determined. The influence of the fineness of the mesh on the results and the modelling of PMMA under impact have been discussed.

[1]On leave from the Department of Solid Mechanics, Technical University of Liberec, The Czech Republic

1 Introduction

The analysis of dynamic fracture is extremely difficult due to the complexity of the problem. Analytical solutions for crack propagation in elastic continua have already been given by Yoffe (1951). Although the analytical solutions are essential for the investigation of various features of dynamic crack propagation, their applicability is restricted to a class of problems with special boundary conditions. Therefore, numerical methods are used for the analysis of real structures, in particular the finite element method (FEM). The crack tip motion is modeled either by a special singular element technique or by a separation of element edges, the so-called "nodal release technique". The first method requires a continuous change of discretization at the crack tip which increases the computational cost considerably. An implementation of the second method is usually easier and introduces no inhomogenities which could become a source of false reflections of stress waves. However, in both methods still two ways can be used to model crack propagation. Firstly, it is possible to prescribe the crack tip velocity and investigate the stress field around the crack by some parameters, e.g. a stress intensity factor $K_{Id}(t)$ as done by Knauss and Losi (1993). Secondly a criterion that controls crack propagation can be defined. In the case of a singular element technique the criterion based on the dynamic fracture toughness K_{ID} is often used, whereas a "nodal release technique" usually prescribes a force behaviour during the node releasing. Here, we use the *discrete crack* model for the modeling of crack initiation and crack propagation through the viscoelastic material under dynamic loading.

2 Discrete crack model

Analysing the constitutive behaviour of a deformation-controlled uniaxial tensile test of concrete a few features can be distinguished. At first, the response of the material is elastic and a linear load-deformation relation almost up to the peak load is observed. At macro-level stress and strain are uniformly distributed within the material and the load-deformation relation for the specimen can

therefore directly be replaced by a stress-strain relation for the material. At the peak load the strain starts to localize within a narrow zone of microcracks (fracture process zone), after which a continuous macrocrack develops. The transferred load decreases with an increasing deformation of the fracture process zone. As a result of this load reduction, the material outside this zone unloads. Due to the fact that the deformation in the descending branch is build up by the straining of the uncracked material and the crack opening the stress-deformation diagram can be split up into a stress-strain relation for the material outside a fracture process zone, and a stress-crack opening relation for the crack itself.

Recognizing this behavior, Hillerborg et al. (1976) proposed the *fictitious crack* model on a basis of the local strength criterion and the fracture mechanics energy balance approach. The model starts from the assumption that in the vicinity of the tip of a visible crack a process zone develops where the strain is beyond the elastic ultimate strain, i.e., where the material already softens. The crack is assumed to propagate when the stress at the crack tip exceeds the tensile strength f_t. When the crack opens the stress is not assumed to fall to zero immediately, but decreases with increasing crack width w. This behaviour is described by a stress-crack opening relation $\sigma(w)$ commonly called a *softening function.* At the critical crack width w_c the stress has decreased to zero. The amount of energy absorbed by increasing the crack width from zero to w_c corresponds to the area under the softening function. This is the energy absorbed per newformed unit crack area and considering the energy balance approach we can choose the softening function so that

$$\int_0^{w_c} \sigma(w)\, \mathrm{d}w = G_c\,. \tag{1}$$

The physical notion of the model is that the area controlled by the softening function in reality corresponds to a microcracked zone with some remaining ligaments for stress transfer.

The softening function is a basic ingredient of the model. Originally Hillerborg (1976) proposes only simple functions for the description of softening behaviour of the material. E.g. if the constant function $f_t = \sigma_y$ and $w_c = \mathrm{COD}$ (Crack Opening Displacement) is chosen the nodel exactly corresponds to the Dugdale model (1960)

for a crack in an elastic - perfectly plastic material. For brittle materials the linear softening function

$$\sigma(w) = f_t\left(1 - \frac{w}{w_c}\right) \qquad w_c = \frac{2G_C}{f_t} \tag{2}$$

can be used. In section 5 bilinear and exponential softening functions will be used for the reproduction of the post-peak response of PMMA.

The discrete crack approach is implemented into finite element codes by means of interface elements. The formation of localized deformation is produced by a separation of the element edges. The constitutive relations of a separation are based on the softening function and are described within the interface element. The formulation of such interface elements is given by Schellekens and de Borst (1994).

3 Description of the experiments

The experiments have been carried out at the Technical University of Liberec. The experimental set-up is shown in Fig. 1. To initiate the crack, the regime of gradual loading of the tested specimen cannot be used, because the experimental device works with a mirror type speed camera and therefore the controlled process must be started by the camera at a suitable moment. This is the reason why a nonstandard specimen geometry has been used.

The plates were preloaded between 7-9 kN and the crack was started by a pressure pulse excited by an explosive wire placed at the end of the transfer bar. The wire explodes due to an instant discharge of a capacitor into the wire placed in the hole of a shaping cube.

The photorecording of the process of fracture of the tested plate enables us to evaluate the crack length - time dependence and the fracture parameters K_I, K_{II}, by means of the field of isochromatic lines. From the crack length - time dependence, the crack propagation velocity was determined. Independent of the photorecording of the plate fracture, four semiconductor strain gauges scan the time behaviour of the stress pulse, both in the transfer bar (gauges T1 and T2) and in the plate (gauges T3 and T4) (see Fig. 1).

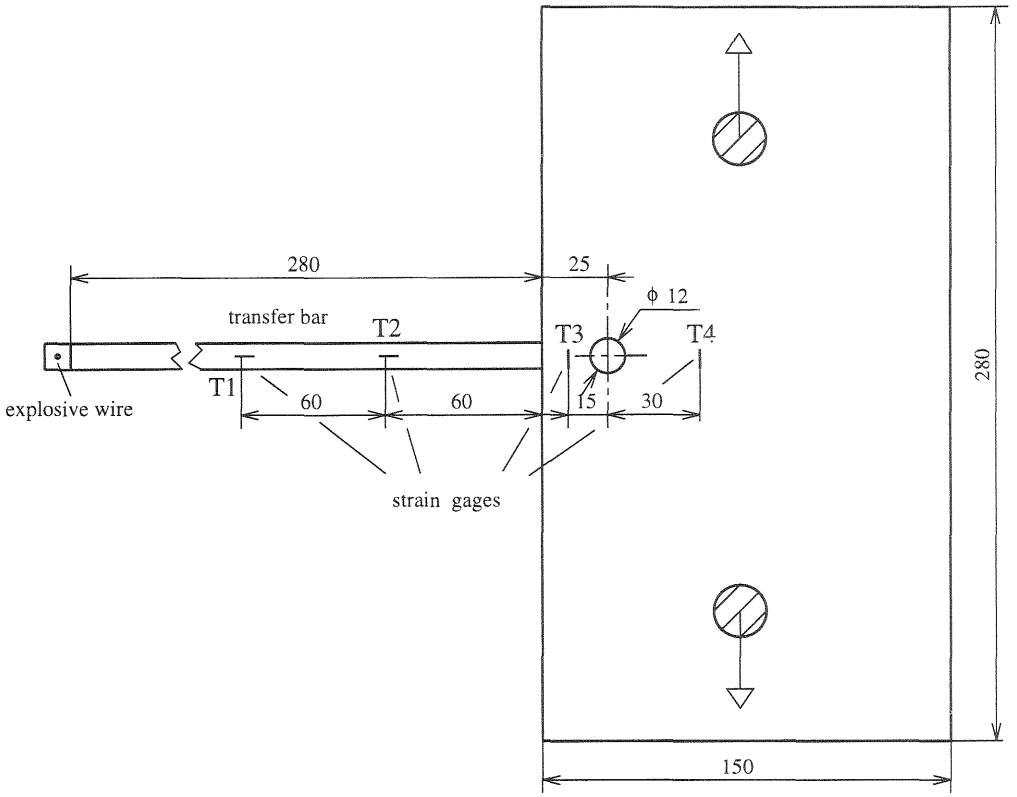

Figure 1: Plate (G-type) with a hole

The experiments were originally used to investigate the dependence of the stress intensity factor $K_{Id}(t)$ on the crack velocity v.

4 The finite element model

Symmetry conditions enables us to consider only half of the plate. The quadrilateral 4-noded isoparametric plane-stress elements with a four-point Gaussian integration scheme has been used. At the axis of symmetry linear interface elements with a Lobatto integration rule have been used to model the prescribed crack path. An initial dummy stiffness was given to the interface elements to avoid additional deformations before cracking. The post-peak behavior of the interface elements was determined by a linear softening relation (cf. eqn.(2)). Only mode I effects have been considered in the analysis. To study mesh sensitivity of the solution two finite element configurations have been used. A coarse mesh with 746 continuum

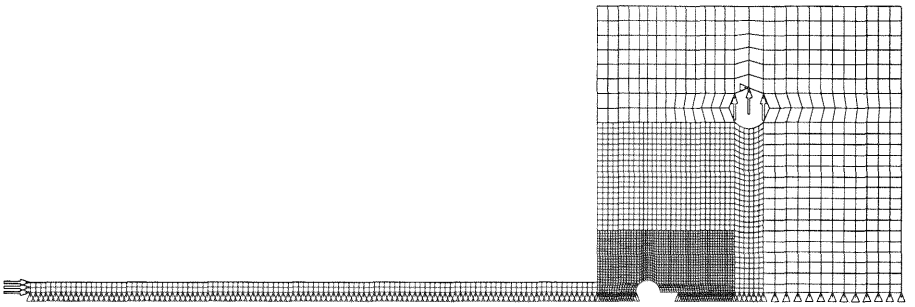

Figure 2: Finite element discretization of the plate - fine mesh (f)

elements and 23 interface elements and a fine mesh with 2700 continuum elements and 49 interface elements have been analysed (see Fig. 2).

Displacement constraints were applied at the axis of symmetry to impose symmetry conditions. Forces applied at the nodes in the grip hole ($\Sigma F_i = 9.0$ kN) produced tensile preloading. The time integration of the field equations has been done using a Newmark scheme ($\delta = 0.5, \alpha = 0.25$) with a time step $\Delta t = 1\mu$s. A consistent mass matrix has been used. The following parameters have been used as material properties (Humen (1993)):

static modulus of elasticity	-	$E_s = 3.5$ GPa,
dynamic modulus of elasticity	-	$E_d = 5.5$ GPa,
Poisson's ratio	-	$\mu = 0.33$
density	-	$\rho = 1180$ kg.m^{-3}
viscosity	-	$\eta = 8400$ s^{-1}
energy release rate	-	$G_{IC} = 310$ J/m^2

The dynamic viscoelastic behavior of PMMA has been modeled using the Maxwell chain model of the material with two units. One chain with the static modulus of elasticity E_s and the other chain with modulus $E_d - E_s$ and a dashpot with viscosity η, placed in serial.

First, the stress intensity factor for the statically preloaded plate was calculated. The output value $K_I^{stat} = 1.19$ MPa$\sqrt{\text{m}}$ is close to the PMMA fracture toughness $K_{IC} = 1.3$ MPa$\sqrt{\text{m}}$, which indicates that the way of preloading causes a situation close to crack initiation in the specimen. This is necessary for dynamic phenomena when the crack is initiated by an external stress pulse as it is with the

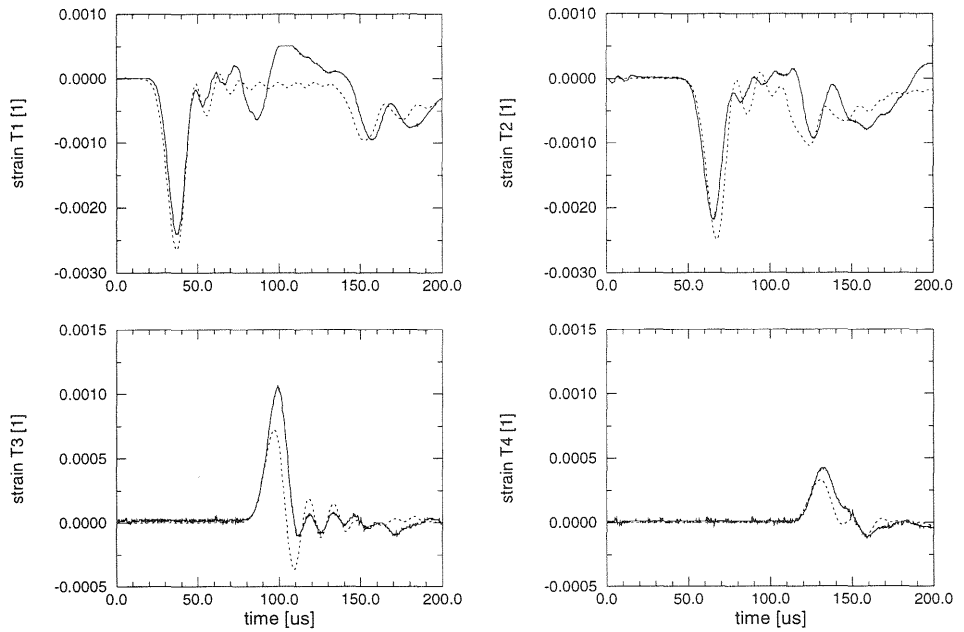

Figure 3: Strain in the T1 - T4 measuring points

LEM experiments. The corresponding tensile stress in the interface element, where the crack tip was situated, was $f_0^{(c)} = 12.24$ MPa for the coarse mesh (c) and $f_0^{(f)} = 23.80$ MPa for the fine mesh (f), respectively.

In an early stage of the test the stress pulse propagation was verified by a comparison with experimental values of the strain. A pressure pulse of 10 MPa amplitude, time length 30 μs and a shape of $sin^2(\omega t)$ was applied to initiate crack propagation. Fig. 3 shows the history of the strain in the T1 - T4 measuring points. Similar results have been obtained for the two different finite element meshes. A good agreement of calculated (a dotted line) and experimental (a solid line) data demonstrates the correct state of stress and strain just before the initiation of crack propagation.

5 Discussion of results

In the calculations the influence of three main parameters of the discrete crack approach, namely the fracture energy G_f, the tensile strength f_t and the shape of the softening function on the crack velocity was tested. The size of the elements near the crack path

Table 1:

mult. fact.	G_f J/m^2	$f_t^{(c)}$ MPa	$f_t^{(f)}$ MPa
0.96	298	13.0	25.3
1.00	310	13.5	26.2
1.02	316	13.7	-
1.04	322	14.0	27.2
1.08	335	-	28.3

was also considered. The results have been compared with the experimental data.

The following approximations based on linear-elastic considerations have been used as the reference values:

$$G_f = G_{IC} \ , \ f_t^{(i)} = f_0^{(i)} \frac{K_{IC}}{K_I^{stat}} \qquad i = \{c, f\} \ , \tag{3}$$

where $K_I^{stat}, f_0^{(c)}$ a $f_0^{(f)}$ are the output from a static stress intensity factor calculation on the corresponding mesh. The estimate of the tensile strength depends on the discretization and it is necessary to evaluate it for a given mesh. The particular reference values (mult.fact.=1.0) as well as their variations have been shown in table 1.

Using the cohesion concept for fracture a question arises: Is the crack tip position at the beginning of the cohesive zone or at the end? In the first case the crack tip position is recorded when the tensile strength in a node is reached. In the second case the time is recorded when a node is released completely. To study the difference between these two crack length definitions both methods have been used. In all figures the results of the first method are plotted at the left, denoted as crack length 1, while results for the second method (crack length 2) are plotted at the right.

The crack length - time relationship was used to compare the influence of the model parameters. The beginning of the stress pulse propagation in the transfer bar was taken as the time origin. The experimental data from the set up only gives relative time information about the crack tip position. To compare this with the numerical

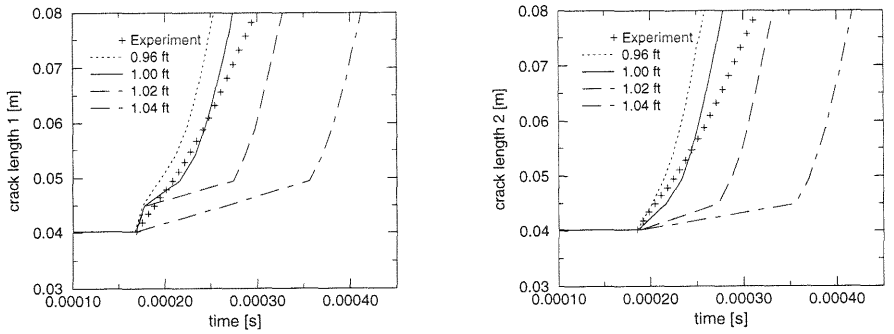

Figure 4: Variation of the tensile strength f_t - coarse mesh

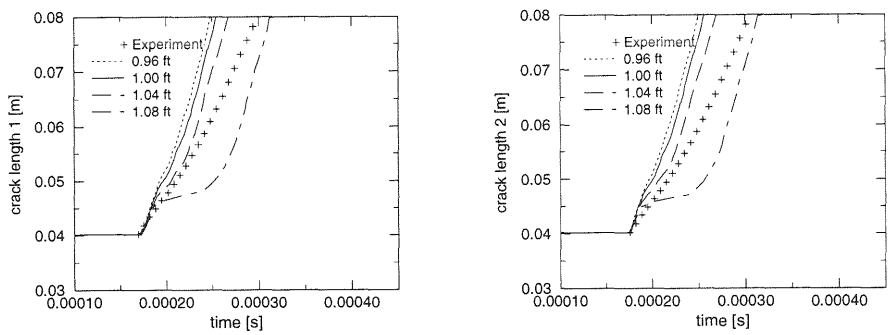

Figure 5: Variation of the tensile strength f_t - fine mesh

results these were shifted in time such that the extrapolated start-point of crack propagation from the experiment coincided with the start of the crack using the reference parameter set.

The resulting crack length - time relationships for different choices of the tensile strength f_t are shown in figures 4 (coarse mesh) and 5 (fine mesh). To enable a comparison between coarse and fine mesh the tensile strength f_t is given with respect to the reference tensile strength $f_t^{(i)}$ (see Tab. 1). As shown in the figures, the change of the tensile strength strongly influences the starting moment of crack propagation. In the steady crack propagation stage the resulting crack velocity is almost insensitive with respect to the discretization and the tensile strength. The crack length - time relationships coming from the different crack tip definitions almost coincide for the fine mesh. It means that the size of the cohesive zone is small with respect to the crack length. The fine mesh is also less sensitive a variation of the tensile strength.

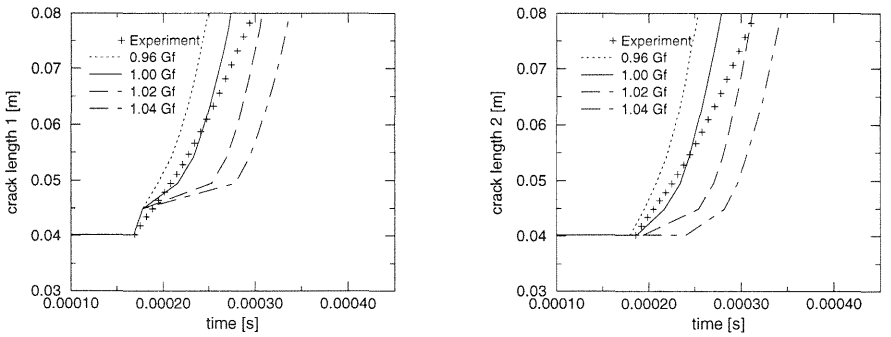

Figure 6: Variation of the fracture energy G_f

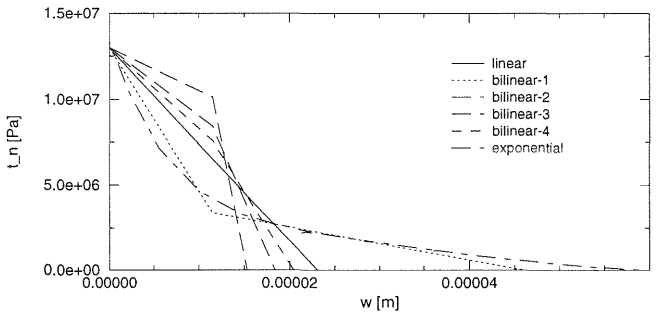

Figure 7: Analysed softening functions

In Fig. 6 the crack length - time relations for a variation of fracture energy G_f under the reference tensile strength $f_t^{(c)}$ have been presented if the coarse mesh is used. Again, we can only observe the influence on the starting phase of the crack propagation. The sensitivity to the method of evaluation is almost the same as in the tensile strength variation. Consequently, the change of the fracture energy influences the cohesive zone formation more than the propagation of it.

In all previous analyses the linear softening function was used. Because the shape of the softening curve for the material was not known, the sensitivity of it on the numerical results has been tested. The softening diagrams are shown in Fig. 7. In addition to the linear function the bilinear function and the exponential softening function according to Reinhard et al. (1986) have been analysed. The point at which the softening modulus is changing,(i.e. $[w_n; t_n]$,

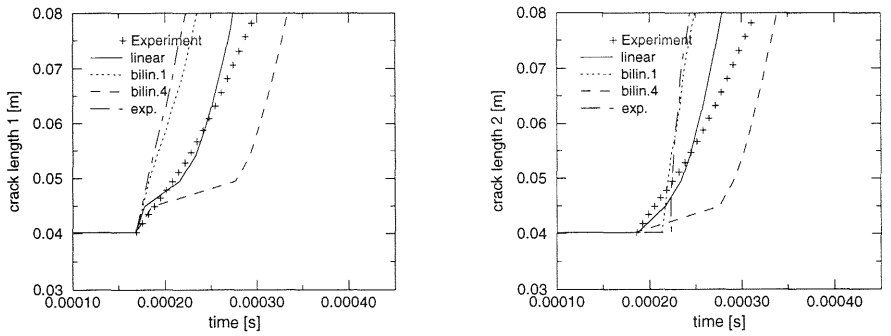

Figure 8: The influence of the softening function

where $w_n = G_f/f_t$) has been varied according to

$$\frac{t_n}{f_t} = \frac{1}{4}\ (\text{var.1});\ \frac{3}{4}\ (\text{var.2});\ \frac{5}{8}\ (\text{var.3});\ \frac{9}{16}\ (\text{var.4}).$$

The other parameters of the curve have been evaluated to keep the fracture energy and the tensile strength at their reference values f_t and G_f. The strong influence of the different softening functions on the crack length - time relationships is shown in Fig. 8. For the variations 2 and 3 the crack did not propagate at all due to unloading in the first part of the bilinear softening characteristic. This result confirms the sensitivity of the results to the initial slope of the softening function.

All investigated parameters, fracture energy G_f, tensile strength f_t and the shape of the softening function, influence the initial stage of crack propagation. In the steady propagation phase the influence of the parameter variation was negligable. The velocity observed in the experiments was smaller for the final stage of fracture. Because the velocity of the crack can not be simulated correctly in the complete time spawn by parameter variation the question arises: How should we modify the model to predict crack propagation in the final stage adequately? It is possible that values for the fracture energy, tensile strength or shape of the softening curve are not constant along the crack path. From the experimental results it can be seen that a more ductile model is needed in the final stage to slow down the crack speed while application of this results in poor results for the initial stage of crack propagation (see Fig. 4). One can conclude that improvement in the description of dynamic crack

propagation can be achieved if the parameters change during propagation of the crack, e.g. if they are rate dependent. A second argument can be the experimental evidence of the $f_t(\dot{\varepsilon})$ dependence for different types of material (e.g. Rossi et al. (1994), Böhme et al. (1992)) as well as successful application of a rate dependent crack model in a continuum-framework in dynamic failure analyse (e.g. Sluys (1994), Sluys and de Borst (1992)).

6 Conclusions

In this paper the discrete crack model for simulation of fast crack propagation in the PMMA plates was used. The initial stage of crack propagation is very sensitive to *(i)* the tensile strength f_t, *(ii)* the fracture energy G_f and *(iii)* the shape of the softening diagram, while during the propagation this sensitivity disappears. The choice of the tensile strength on the basis of fracture toughness K_{IC} appeared to be successful for the description of the dynamic crack propagation.

Acknowledgements

The computations in this paper have been performed using the DIANA finite element package of TNO Building and Construction Research. The financial support of the study by Delft University of Technology is gratefully acknowledged.

References

Böhme, W., Sun, D.Z., Schmitt, W. and Höning, A. (1992) Application of micromechanical material models to the evaluation of Charpy tests, in **Advances in Fracture/Damage Models for the Analysis of Engineering Problems**, AMD 137, ASME, 203-216.

Dugdale, D.S. (1960) Yielding of steel sheets containing slits. **J. of Mech. and Phys. of Solids**, 8, 100-108.

Hillerborg, A., Modéer, M. and Petersson, P.E. (1976) Analysis

of crack formation and crack growth in concrete by means of fracture mechanics and finite elements. **Cement and Concrete research**, 6, 773-782.

Humen, V. and Potěšil, A. (1993) Pulse method used to identify material properties in linear viscoelastic media. **Int. J. of Impact Engng**, 13(1), 85-98.

Knauss, W.G. and Losi, G.U. (1993) Crack propagation in a nonlinearly viscoelastic solid with relevance to adhesive bond failure. **J. Applied Mech.**, 60, 793-801.

Reinhard, H.W., Cornelissen, H.A.W. and Hordijk, D.A.(1986) Tensile tests and failure analysis of concrete. **J. Struct. Engng**, 112(11), 2462-2477.

Rossi, P., van Mier, J.G.M., Toutlemonde, F., Le Maou, F. and Boulay, C. (1994) Effect of loading rate on the strength of concrete subjected to uniaxial tension, **Materials and Structures**, 27, 260-264.

Schellekens, J.C.J. and de Borst, R. (1994) The application of interface elements and enriched or rate-dependent continua to micromechanical analyses of fracture in composites. **Computational Mechanics**, 14, 68-83.

Sluys, L.J. (1994) Gradient theory : Discretization principles and application, in **Computational Modeling of Concrete Structures** (eds. H. Mang, N. Bićanić, R. de Borst), Pineridge Press 1994, 403-412.

Sluys, L.J. and de Borst, R. (1992) Analysis of impact fracture in a double-notched specimen including rate effects, in **Fracture Mechanics of concrete structures** (ed. Z.P. Bažant), Elsevier, N.Y., 610-615.

Yoffe, E.H.(1951) The moving Griffith crack, **Philosophical Magazine**, 42, 739-750.